Mass transport using the series of vortex rings with swirl

Takashi NAITOH*, Nobuyuki OKURA** and Osamu SUMITOMO*
*Graduate School of Engineering, Nagoya Institute of Technology
Gokiso-cho, Showa-ku, Nagoya 466-8555, Japan
E-mail: naitoh.takashi@nitech.ac.jp
**Department of Vehicle and Mechanical Engineering, Meijo University
1-501 Shiogamaguchi Tempaku-ku, Nagoya, 468-8502, Japan

Abstract
Behavior of the series of laminar vortex rings with circumferential flow, so-called swirl, were investigated using flow visualization, to evaluate the transport efficiency of the ejected fluid as vortex rings. In this study, the interval time of the vortex ring ejection, the formation number of vortex ring L_O/D_O (the normalized length of the ejected slug of fluid), and the angular velocity of the ejected fluid ω are changed, while the mean ejection velocity is fixed. When vortex rings were generated at a short time interval, independent of L_O/D_O and ω, they were broken, and most of the fluid included in them was diffused near the orifice. When the vortex rings with little mutual interference were generated at an appropriate interval time, the breakdown of vortex ring structure is suppressed with moderate swirling flow. In those cases, each vortex ring moves separately for a long distance and the distribution area becomes wider as L_O/D_O increases.

Keywords : Vortex rings, Swirl, Mass transport, Formation number, Flow visualization

1. Introduction

Since a vortex ring has continuous translational movement as a compact solitary wave and exchanges less fluid between the inside and outside of the vortex ring, there is less fluid left in its path. That is, the vortex ring has strong directionality, and can be expected to transport fluid in a region away from the outlet. It is therefore worth examing the ability of the vortex ring to transport fluid to a specific small region in free space. Additionally, since there are various parameters for vortex ring formation and many patterns of interference between vortex rings, it is possible to control the transport characteristics by the optimal combination of formation parameters and interference pattern. Transfer efficiency and energy conservation can be improved if the diffusion of fluid in unintended regions can be reduced by transporting fluid via vortex rings. Significant cost reduction can also be expected if the fluid to be transported is expensive.

Domon et al., (2000) reported an experiment on material transport using a high Reynolds number vortex ring. Since the specific gravity of the particles is slightly variable and the particle diameter was not too small to follow the flow, those particles with a specific gravity greater than unity are spun off from the vortex ring via centrifugal force at an early stage and the remaining particles are carried to the end of the water tank. As a result, it became clear that the specific gravity of the material to be transported must be less than that of the fluid composing the vortex ring.

Naitoh et al., (2011) investigated the use of the series of vortex rings to transport a small amount of fluid by discharging a relatively moderate flow so as to obtain a high density distribution of the fluid in a specific narrow region. They quantitatively analyzed the distributions of transported fluid in two cases when vortex rings were formed by 10 to 20 ejections of fluid compared to a single, short puff-like ejection with the total volume of ejected fluid being constant in both cases. Their results showed that the vortex rings is superior to the single short ejection for transporting fluid to obtain a high-density distribution in a narrow region.

A laminar vortex ring may go through four stages of development: the generation process, the stable laminar phase, the unstable or wavy phase, and the turbulent phase (Lim and Nickels, 1995). When a laminar vortex ring becomes

turbulent, the propagation velocity decreases abruptly. However, the swirling flow in a vortex ring core reduces the amplification rate of the azimuthal wavy deformation and preserved its ring structure (Yajima and Gotoh, 1996; Naitoh et al., 2007). Then the traveling distance of a vortex ring can be extended using the swirling flow under certain conditions. The effects of swirl on the dynamics of a vortex ring were investigated theoretically and numerically (Moffatt, 1988; Grauer and Sideris, 1991; Pumir and Siggia, 1992; Virk *et al*., 1994; Hu et al., 2001; Chen et al., 2010). From the viewpoint of flow control on a laminar vortex ring, the swirling flow rate is one of the most expected generation parameters of a vortex ring.

The primary goal of this study is to investigate the fluid distribution transported by the series of vortex rings with swirl. In particular, we focus on three generation parameters: the interval time of the vortex ring ejection, the formation number of vortex ring L_O/D_O (the normalized length of the ejected slug of fluid defined by Gharib et al., 1998), and the angular velocity of the outlet Ω, while the mean ejection velocity is fixed.

2. Experimental setup and generating parameters of vortex ring

2.1 Experimental setup and procedure

Figure 1 shows the experimental apparatus. The water tank is 1,480 mm long, 480 mm wide, and 490 mm high. An acrylic resin cylinder, which has an inner diameter of 50.0 mm, is installed at the center at one end of the water tank. Vortex rings are generated by pushing the fluid inside the cylinder via a piston. A linear motor configured by a stepping motor and rack-and-pinion mechanism drives the piston. The movement of the piston is controlled by pulse signals generated by a PC. The circular pipe made of PVC resin (inner diameter = 40.0 mm, length = 153 mm) attached with the orifice were inserted to the acrylic resin cylinder and held with two bearing stands which are omitted in Fig. 1 to avoid confusion. The orifice diameter (D_O) was 20.0 mm, and it was defined as a representative length scale. A timing pulley was set up between the bearing stands, and the stepping motor above the tank could rotate the PVC resin pipe by using a timing belt. The pipe has been rotating for 15 seconds, and by pushing the fluid for a short period of time, the vortex rings with swirl were formed. The dividing screen which shields the test section from the disturbance due to the movement of the timing belt was laid on and only the tip of the PVC pipe attached with the orifice was exposed to the test section through a circular hole on the screen. Figure 1 also defines the cylindrical coordinate system used for this experiment. θ defines rotation counter-clockwise, however, the angular velocity of the PVC resin pipe (Ω) is measured clockwise. The two types of elapsed time, "t" and "t^*," are defined as the time from the beginning of fluid ejection and its completion, respectively.

Fluorescent dyes were premixed in the cylinder using a syringe several minutes prior to actuating the cylinder. The syringe had a narrow 70-cm-long nozzle to avoid disturbing the fluid within the water tank. The flow field was lighted by a 650 W halogen lamp with a lens system mounted on one side of the water tank during the flow visualization experiments. The camera was positioned to capture images lateral to the flow direction. The photographic time interval was 1.0 seconds.

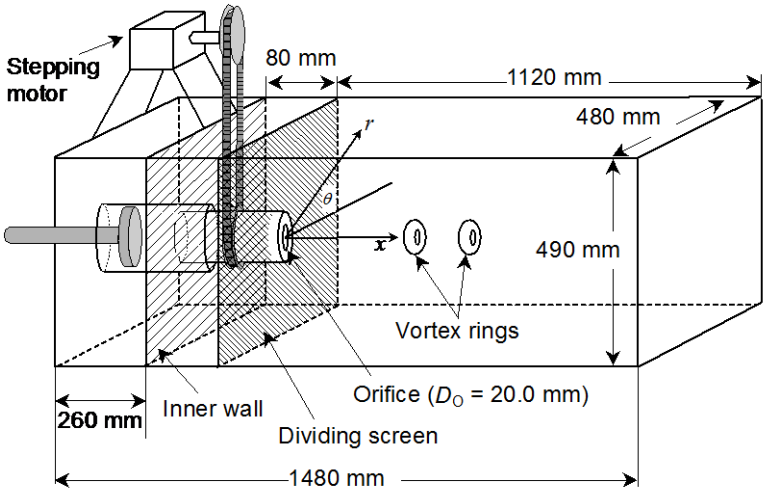

Fig. 1 Experimental apparatus.

2. 2 Generating parameters of vortex ring

The purpose of this experiment was to investigate the features of fluid distribution when it is ejected from the cylinder in accordance with the ejecting parameters. Although there are many choices of parameters, we paid attention to the thickness of a vortex ring, strength of swirling flow, and time interval of fluid ejection. Thus, we chose the three cases of piston stroke length (L_p) shown in Table 1 and four kinds of interval time (Δt) in case B. The circulation of a vortex ring Γ_{slug} estimated using a slug model is .

$$\Gamma_{slug} = \int_0^T \frac{1}{2} U_o^{\,2}(t)dt \qquad (1)$$

where T is duration time of fluid ejection and U_O is the averaged ejection velocity. These experiments are carried out under the condition, $L_O/D_O < 4$, thus the value of Γ_{slug} is estimated assuming that all the discharged circulation of the free shear layer during the one ejection is accumulated in the vortex ring. The piston velocity (U_p) and the total piston stroke length are fixed at 20.0 mm/s and 40.0 mm, respectively, in all cases, i.e., the volume of the ejection fluid is 78.5 cm^3. The speed of piston movement was set to be constant. Actually, each of the acceleration and deceleration periods of the piston movement was measured as 3 ms by means of the examination of images captured by the high-speed camera. When the piston moves the distance L_P = 4.0 mm with the speed U_P = 20.0 mm/s, the total period for acceleration and deceleration, 6 ms, is only 3% of the piston movement time, 200 ms. Then, the total momentum of the fluid ejection in each case is almost the same.

A dimensionless parameter called swirl number, S is defined by Chen et al., 2010 as

$$S = \frac{U_S R_S}{\Gamma_S} \qquad (2)$$

where U_S is the maximum swirl velocity around the azimuthal axis of the ring localized inside the core, R_S is the radius of the ring, and Γ_S is the circulation of the ring. Although it is difficult to accurately estimate a swirl number, we inferred it for Case B at Ω = 0.2 π [rad /s] as the representative case in accordance with equation (2) in the following way. Since the inner diameter of the rotating PVC resin pipe is twice the diameter of the orifice, the possible maximum velocity of U_S is 1.2 cm/s. By assuming that R_S = 1.0 cm which is the radius of the orifice and Γ_S is adopted from Γ_{slug}, S is estimated at 0.8×10^{-1}.

Table 1 Experimental conditions.

Case	L_P [mm]	Number of ejection	L_O/D_O	Re $= \Gamma_{slug}/\nu$	Ω [rad/s]	Δt [s]
A	2.0	20	0.63	0.8 x 10^3	0.0 π, 0.2 π, 0.5 π	5.0
B	4.0	10	1.25	1.6 x 10^3	0.0 π, 0.2 π, 0.5 π	1.0, 3.0, 5.0, 10.0
C	6.0	7	1.88	2.3 x 10^3	0.0 π, 0.2 π, 0.5 π	5.0

3. Mutual interference of vortex rings: effect of swirling flow

3.1 Vortex rings without swirl

The interactions between vortex rings in case B (Δt = 5.0 s) are observed in detail as a representative (typical) flow pattern among three cases. Figure 2 primarily shows the interactions of vortex rings without swirl in comparison with those with swirl. Each picture has a sequence of marks at regular intervals of $2D_O$ on its bottom.

An azimuthal wavy deformation as shown in Fig. 3 (a) appears in all vortex rings when they arrive at about x/D_O =12. As for the first vortex ring, it becomes turbulent at about x/D_O =15 (Fig. 3 (b)) and its velocity decreases, and then it goes back to a laminar circular vortex ring (Fig. 3 (c)) due to viscous dissipation and slowly moves toward downstream (Fig. 2, t = 10 s). The second vortex ring approaches the preceding vortex ring because of its velocity reduction. The structure of the second vortex ring is completely broken at about x/D_O = 24, and the ejected dye contained in the second vortex ring diffuses in the surrounding area. (Vortex rings except for the first one do not form circular rings again after breaking.) Thereafter, the following vortex rings are broken one after another at the same position and the region which the dye diffuses in slowly moves toward downstream (Fig. 2, t = 50 s). The position of

the vortex ring breaking determines the distance of dye distribution area from the orifice, so that, the distribution area is limited in a narrow range. The dye diffused region came to a standstill soon after all of the vortex rings merged into its region.

3. 2 Vortex rings with swirl (Ω = 0.2π rad/s)

The previous studies (Kato et al., 2009; Naitoh et al., 2007) found the nature of vortex rings with swirl as follows. 1) The thickness of a vortex core with swirl becomes thin relative to that without swirl. 2) The swirling flow in a vortex ring core reduces the amplification rate of the azimuthal wavy deformation. 3) A vortex ring with swirl is insensitive to disturbances since the swirling flow preserves its ring structure. 4) Then the temporal decrease of the propagation velocity of a vortex ring with moderate swirl is small.

Figure 4 shows the successive visualization of vortex rings with swirl (Ω = 0.2π rad/s, Δt = 5.0 s) in case B. We also observe that the thickness of a vortex core is reduced with increase of angular velocity Ω in this study. The space between vortex rings with swirl (Ω = 0.2π rad/s) at t = 10 s and t = 20 s in Fig. 4 is wider than that without swirl in Fig.

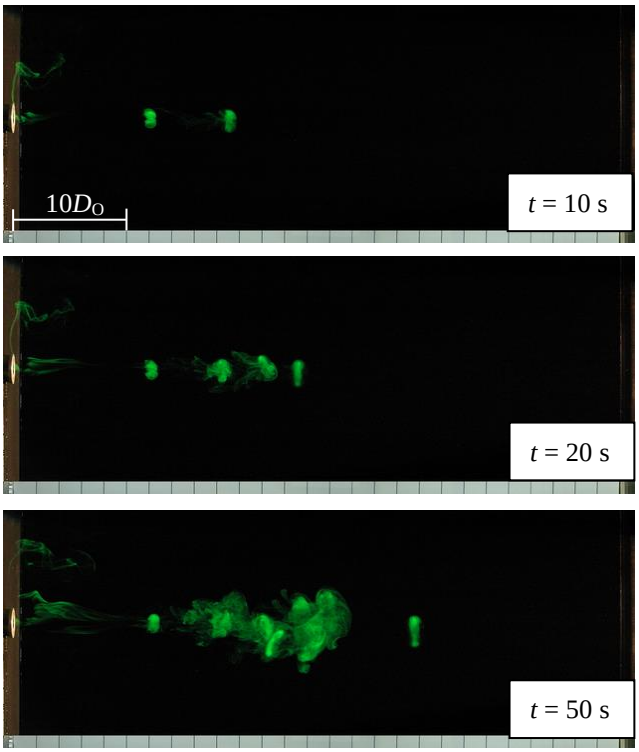

Fig. 2 Successive visualization of vortex rings without swirl in case B.

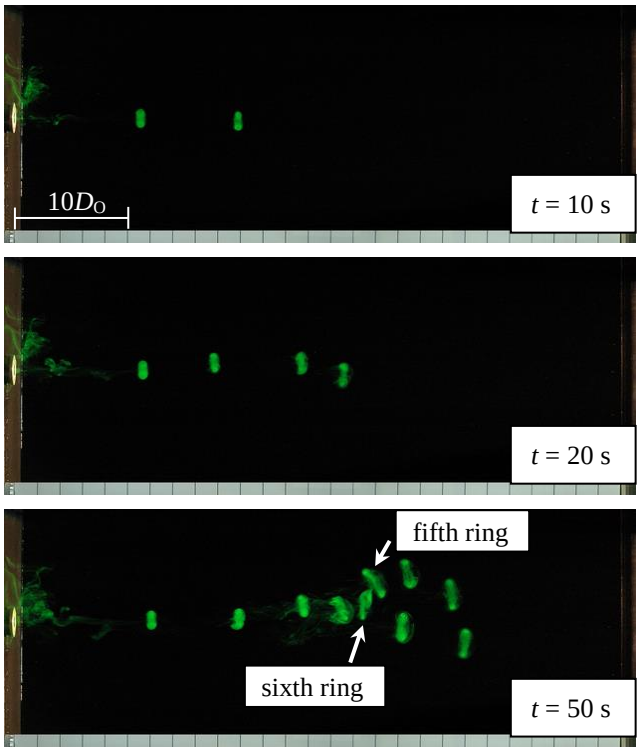

Fig. 4 Successive visualization of vortex rings with swirl (Ω = 0.2 π rad/s) in case B.

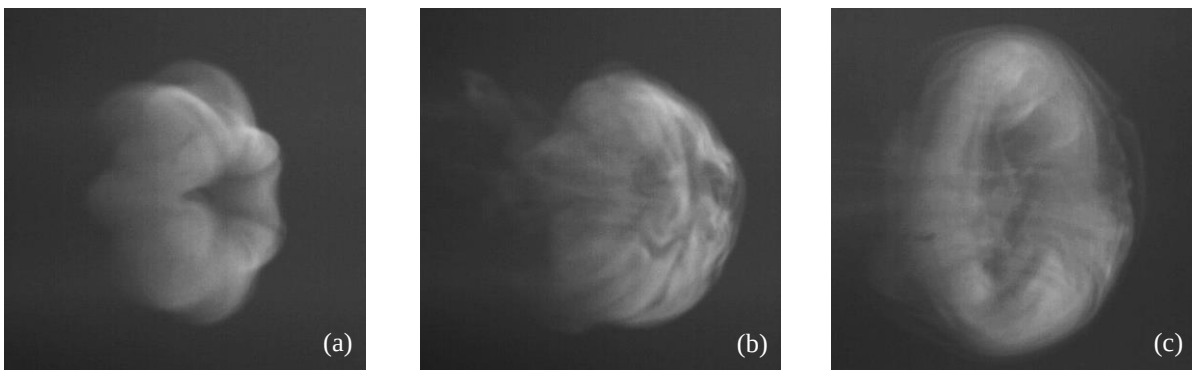

Fig. 3 Visualization of vortex rings without swirl in case B: (a) azimuthal wavy deformation, (b) turbulent state, (c) laminar state.

2, because the decrease of the propagation velocity is small.

The direction of the second vortex ring and the following are slightly deflected by the disturbance which is due to the vorticity left behind the preceding vortex ring caused by the "peeling" (Kato, 2009). The space between vortex rings with swirl (t = 50 s) increases because of the deflection, and the mutual interactions of rings are reduced. Interestingly, the vortex ring does not deflect in the same direction in which the immediately preceding vortex ring moves. Therefore, the disturbance in the wake of the vortex ring with swirl may be developed in some flow structures.

The fifth and sixth vortex rings pointed out in Fig. 4 interact and are mutually deformed at t = 50 s. Soon after the deformation, their propagation velocity in x-direction decreases and the interspaces between vortices become narrow, so that the interaction of vortex rings becomes strong. As seen in the following distribution at t = 125 s (t^* = 80 s) shown later in Fig. 6, the dye fluid transported by the fifth and later vortex rings is finally merged, while that by the first four vortex rings is distributed independently.

3. 3 Vortex rings with swirl (Ω = 0.5π rad/s)

Figure 5 shows the vortex rings with swirl (Ω = 0.5π rad/s, Δt = 5.0 s) in case B. The propagation velocity in each vortex ring decreases and the interspaces between vortices become narrow as compared with those of Ω = 0.2π rad/s in case B. This is because the discharged fluid by the "peeling" increases and its circulation decreases. The increment of the discharged fluid can be confirmed by the high-density distribution of dye between x/D_O = 2 and 6.

The angle of deflection for the condition of Ω = 0.5π rad/s is greater than those of Ω = 0.2π rad/s. Then the interspaces between vortices become wider and the mutual interactions of vortex rings become weak. Because of the weak interaction and the self-preserving nature due to the swirling flow, the merging of vortex rings cannot be seen in Fig. 5.

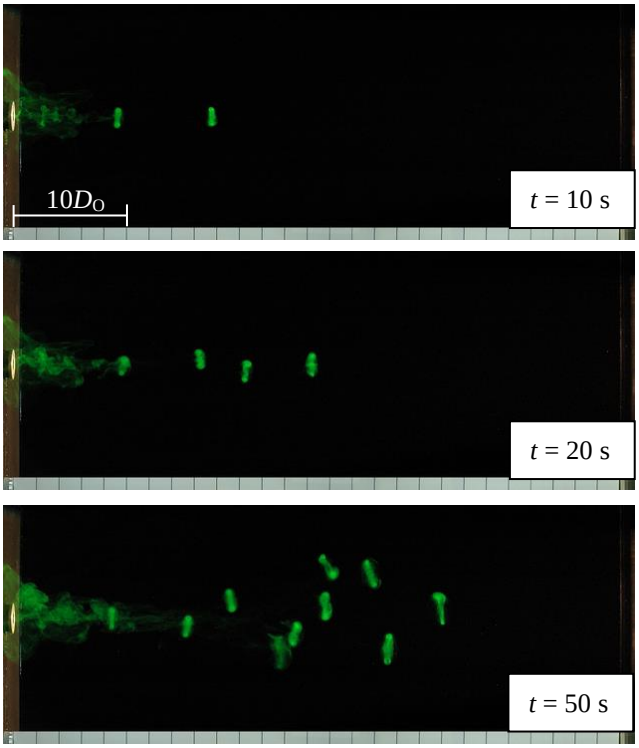

Fig. 5 Successive visualization of vortex rings with swirl (Ω = 0.5 π rad/s) in case B.

3. 4 Distribution of transported fluid

Figure 6 shows the fluid distribution transported by vortex rings with/without swirl at t^* = 80 s in all cases. In case A (L_p = 2.0 mm), the circulation, the propagation velocity, the diameter, the Reynolds number, and the core diameter of

a vortex ring are small in comparison with those in case B (L_p = 4.0 mm), and the traveling distance of a vortex ring is also short. The temporal development of flow field for Ω = 0.0π rad/s in case A is similar to that for Ω = 0.0π rad/s in case B as shown in Fig. 2. On the other hand, because of the small Re and the self-preserving nature of vortex rings with swirl, the vortex rings for Ω = 0.2π rad/s and Ω = 0.5π rad/s maintain the laminar state without transition to turbulence. They come to a stop when the vorticity is dissipated. Therefore, they are distributed in a narrow range.

The traveling distance of an individual vortex ring in case C (L_p = 6.0 mm) may be long relative to those in case A and B. However, the fluid distribution transported by vortex rings for Ω = 0.0π rad/s in case C is dominated by the transition to turbulence and mutual interaction of vortices, and is similar to that for Ω = 0.0π rad/s in case A and B. In contrast, the vortex rings for Ω = 0.2π rad/s and Ω = 0.5π rad/s in case C arrive at the farthest position in the water tank, though some of the rings for Ω = 0.2π rad/s break on the midway.

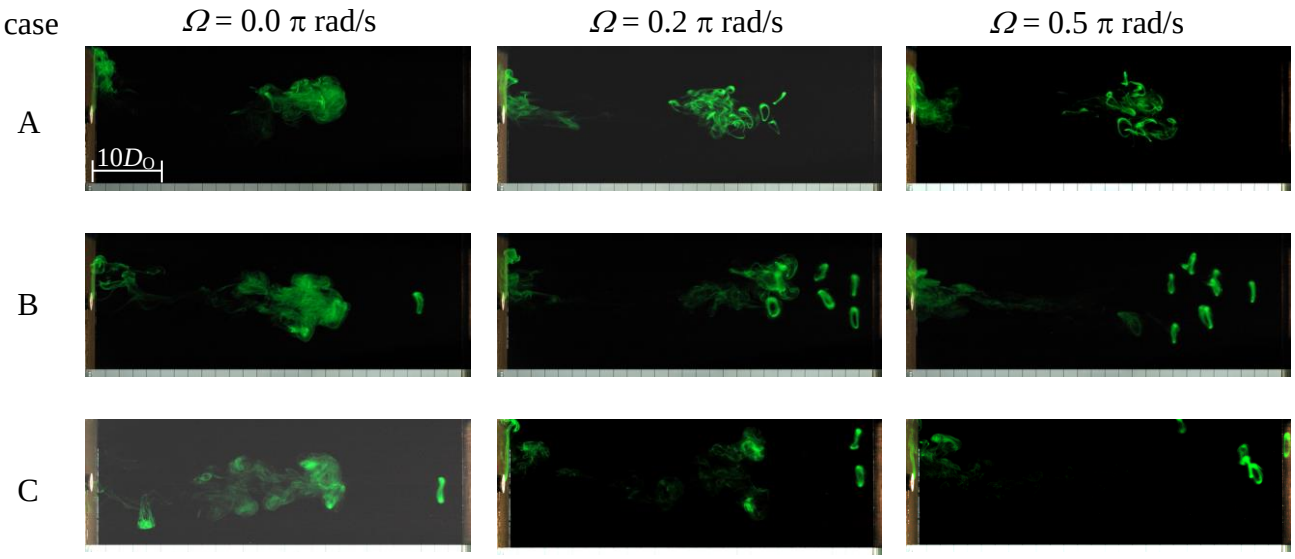

Fig. 6 Fluid distribution transported by vortex rings with/without swirl at t^* = 80 s in all cases.

We classified the appearance of the fluid distribution in three groups. The state that most of ejected fluid is gathered in a small region like Fig. 2 is referred to as a "cluster." As seen in Fig. 5, the state that vortex rings are independently traveling without interaction is referred to as "scatter." And the intermediate state between "cluster" and "scatter," that means some preceding vortex rings are independently traveling and the rest followings are gathered, is referred to as "partial cluster." Table 2 will help to clarify the relation of the state of fluid distribution and generation parameters of vortex rings. From the above, it is found that the mutual interaction of vortex rings can be controlled with generation parameters in Table 1 and the swirling flow is an effective parameter to change the fluid distribution.

Table 2 Classification of fluid distributions

L_P [mm]	Ω = 0.0 π rad/s	Ω = 0.2 π rad/s	Ω = 0.5 π rad/s
2.0	cluster	cluster	cluster
4.0	cluster	partial cluster	scatter
6.0	cluster	partial cluster	scatter

4. Effect of ejection time interval

The time interval of fluid ejection (Δt) is not only a most effective parameter which governs the mutual interaction of vortex rings but also one of the key factors determining the mass flux of ejected fluid from a viewpoint of applications. Figure 7 shows the fluid distribution at t^* = 45 s in case B regarding four kinds of Δt.

As for the condition of Δt = 1.0 s, because of the strong mutual interaction, almost all vortex rings are merged. Even for Ω = 0.5 π rad/s, only the first two vortex rings can escape and move downstream independently.

As Δt increases, the mutual interaction of vortex rings becomes weak and the state of fluid distribution tends to be a "scatter." Moreover, the disturbance on the way of vortex ring produced by the preceding one with swirl becomes less intense. Hence, the angle of deflection for vortex rings with swirl also decreases with increment of Δt.

As compared with the fluid distribution of Ω = 0.2 π rad/s and that of Ω = 0.5 π rad/s for Δt = 3.0 s, it is found that the former shows scatter and the latter partial scatter, though the swirling flow of the latter is stronger than that of the former. This is because the discharged fluid from vortex rings due to "peeling" makes the disturbance intense. Therefore, the optimization of the parameter Ω in each condition is essential to control the fluid transport.

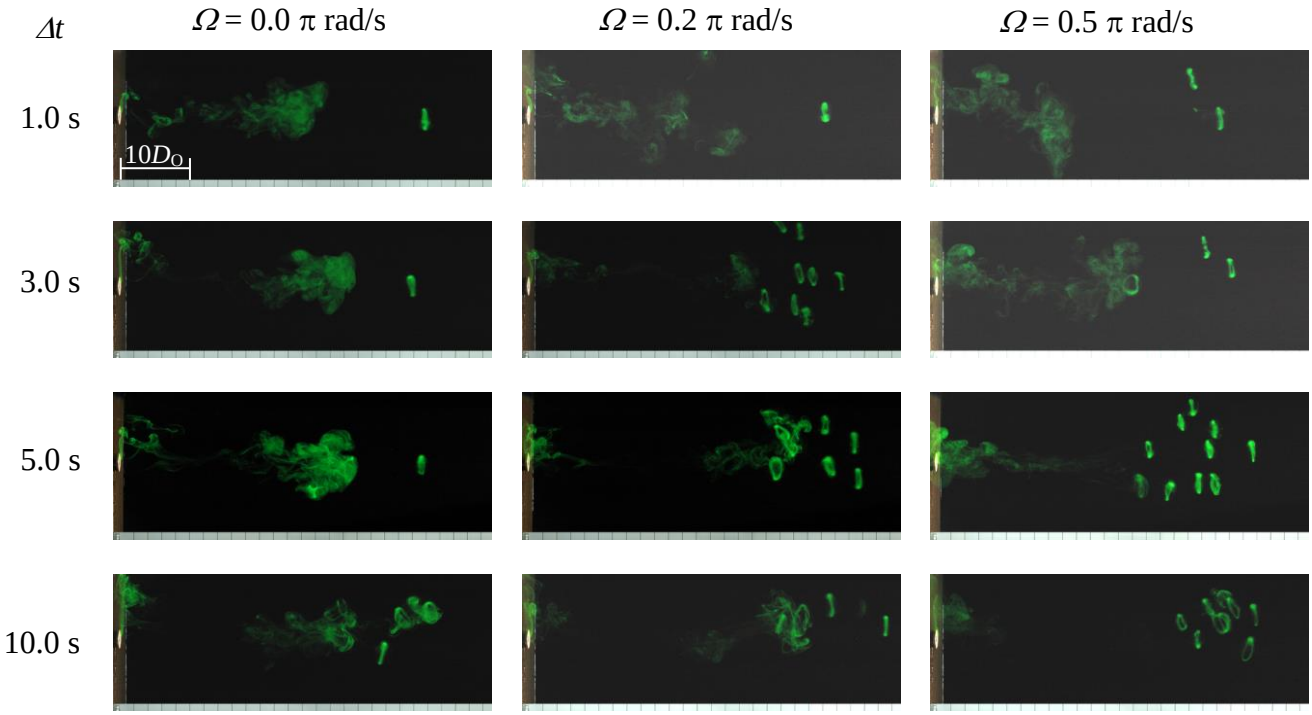

Fig. 7 Fluid distribution transported by vortex rings with/without swirl at t^* = 45 s in cases B.

5. Conclusion

The state of the fluid distribution transported by vortex rings are classified in three groups: "cluster," "partial cluster," and "scatter." Based on this classification, it is easy to summarize the function of each vortex generation parameter for controlling the fluid transportation. Within this experimental condition, each parameter reveals the following trends.

Since the swirling flow in a vortex ring core reduces the amplification rate of the azimuthal wavy deformation and preserves its ring structure, a vortex ring with swirl is insensitive to disturbances. Then when the angular velocity of the orifice (Ω) is moderate, vortex rings are independently traveling without interaction. As the result, the state of fluid distribution tends to be "scatter." But if Ω is too strong in this experimental setup, the discharged fluid from vortex rings due to "peeling" make the disturbance intense and vortex rings tend to be in the state of "cluster."

For a single vortex ring with/without swirl, its traveling distance increases with the increment of the formation number L_O/D_O. Then the distance of fluid transportation increases with L_O/D_O when the state of distribution for vortex rings is scatter. However, when the state of distribution for vortex rings is cluster because of other parameters, the distance of fluid transportation is determined by the position where the vortex rings break.

As for a short time interval of fluid ejection (Δt), vortex rings interacted closely and the state of fluid distribution tends to be cluster. Conversely when the time interval becomes longer, the state of fluid distribution tends to be a "scatter." In addition, the angle of deflection for vortex rings with swirl decreases with the increment of Δt because the

disturbance produced by the preceding one with swirl becomes less intense.

Acknowledgments

This work was supported by JSPS KAKENHI Grant Number 21560169.

References

Cheng, M., Lou, J. and Lim, T. T., Vortex ring with swirl: A numerical study, Physics of Fluids, Vol. 22 (2010), 097101.

Domon, K., Ishihara O. and Watanabe S., Mass transport by a vortex ring, Journal of the Physical Society of Japan, Vol. 69, No. 1 (2000), pp. 120-123.

Gharib, M., Rambod, E. and Shariff, K., A universal time scale for vortex ring formation, Journal of Fluid Mechanics, Vol. 360 (1998), pp. 121 - 140.

Grauer, R. and Sideris, T. C., Numerical computation of 3D incompressible ideal fluids with swirl, Physical Review Letters Vol. 67, No. 25 (1991), pp. 3511 - 3514.

Hu, G. H., Sun, D. J. and Yin, X. Y., A numerical study on vortex rings with swirl, Journal of Hydrodynamics, Series B, Vol. 2 (2001) pp. 1 - 8.

Kato, Y., Naitoh, T. and Okura, N., Observation of vortex ring with swirl by using successive 3-D images, Proceedings of the Japan Society of Mechanical Engineers, Fluid Engineering Conference 2009 (2009) pp. 5 - 6 (in Japanese).

Lim, T. T. and Nickels, T. B., Fluid Vortices (1995), pp. 95-149, Kluwer Academic Publishers.

Moffatt, H. K., Generalised vortex rings with and without swirl, Fluid Dynamics Research Vol. 3 (1988), pp. 22 - 30.

Naitoh, T., Okura, N., Okude M. and Utsumi, Y., Quantitative measurement of mass transport using vortex rings, Transactions of the Japan Society of Mechanical Engineers, Series B, Vol. 77, No. 775 (2011) pp. 557-567 (in Japanese).

Naitoh, T., Okura, N. and Okamoto, H., Behavior of vortex rings with swirl, Proceedings of 2007 Annual Meeting, Japan Society of Fluid Mechanics (2007) p.337 (in Japanese).

Pumir, A. and Siggia, E. D., Development of singular solutions to the axisymmetric Euler equations, Physics of Fluids A Vol. 4, No. 7 (1992), pp. 1472 - 1491.

Virk, D., Melander, M. V. and Hussain, F., Dynamics of a polarized vortex ring, Journal of Fluid Mechanics, Vol. 260 (1994), pp. 23 - 55.

Yajima, M. and Gotoh, T., Instability of a vortex ring, Research Institute for Mathematical Sciences (Kyoto University), Kokyuroku, Vol. 972 (1996), pp. 24 - 34 (in Japanese).